

Characterization of CD8⁺ T Cell Function and Immunodominance Generated with an H₂O₂-Inactivated Whole-Virus Vaccine

Joshua M. Walker, Hans-Peter Raué, and Mark K. Slifka

Oregon National Primate Research Center, Oregon Health & Sciences University, Beaverton, Oregon, USA

CD8⁺ T cells play an important role in protection against both acute and persistent viral infections, and new vaccines that induce CD8⁺ T cell immunity are currently needed. Here, we show that lymphocytic choriomeningitis virus (LCMV)-specific CD8⁺ T cells can be generated in response to a nonreplicating H₂O₂-inactivated whole-virus vaccine (H₂O₂-LCMV). Vaccine-induced CD8⁺ T cell responses exhibited an increased ability to produce multiple cytokines at early time points following immunization compared to infection-induced responses. Vaccination with H₂O₂-LCMV induced the expansion of a narrow subset of the antigen-specific CD8⁺ T cells induced by LCMV strain Arm infection, resulting in a distinct immunodominance hierarchy. Acute LCMV infection stimulated immunodominance patterns that shifted over time or after secondary infection, whereas vaccine-generated immunodominance profiles remained remarkably stable even following subsequent viral infection. Vaccine-induced CD8⁺ T cell populations expanded sharply in response to challenge and were then maintained at high levels, with responses to individual epitopes occupying up to 40% of the CD8⁺ T cell compartment at 35 days after challenge. H₂O₂-LCMV vaccination protected animals against challenge with chronic LCMV clone 13, and protection was mediated by CD8⁺ T cells. These results indicate that vaccination with an H₂O₂-inactivated whole-virus vaccine induces LCMV-specific CD8⁺ T cells with unique functional characteristics and provides a useful model for studying CD8⁺ T cells elicited in the absence of active viral infection.

CD8⁺ T cells are critical in host immune defense against intracellular pathogens by producing antiviral cytokines and eliminating infected cells by perforin- and Fas-mediated lysis (20, 22, 54). Although humoral immunity plays an important role in vaccine-mediated immunity (3), many of the current targets of vaccine development (HIV, hepatitis C, etc.) are viral infections in which an effective CD8⁺ T cell response will likely be important or required for protection. New vaccines that are able to stimulate robust CD8⁺ T cell-based immunity are needed, and their development has the potential to significantly reduce morbidity and mortality associated with a number of important infectious diseases.

Immunodominance is a common feature of CD8⁺ T cell responses and occurs when CD8⁺ T cells are directed against only a small subset of the total possible epitopes within a given pathogen (61). Some peptides induce a higher degree of T cell clonal expansion and/or survival than others, resulting in predictable immunodominance patterns for each combination of pathogen and major histocompatibility complex I (MHC-I) (61). Mechanisms believed to play a role in determining immunodominance include antigen load (28), duration of antigen exposure (62), efficiency of antigen processing and presentation (61), naïve T cell precursor frequency (27), competition between T cells for antigen-presenting cells (24), and the ability of CD8⁺ T cell populations to produce and respond to gamma interferon (IFN- γ) (30, 58).

Commercial inactivated whole-virus vaccines are produced by exposing the virus of interest to a cross-linking agent such as formaldehyde or an alkylating agent such as beta-propiolactone. These approaches may damage immunogenic epitopes during the course of virus inactivation and in some cases may even exacerbate disease outcome following subsequent infection (5, 9, 13, 25). In contrast, we have found that virus inactivation by oxidation with H₂O₂ provides a simple new approach for inducing strong neutralizing antibody responses and effective antiviral immunity (4).

In this study, we have determined how immunization with an H₂O₂-inactivated whole-virus vaccine influences the immunodominance of the resulting MHC-I-restricted CD8⁺ T cell response to lymphocytic choriomeningitis virus (LCMV) in C57BL/6 mice. The immune response to LCMV infection in C57BL/6 mice has been extensively characterized, making it an ideal system to examine vaccine-mediated CD8⁺ T cell responses. LCMV is a natural mouse pathogen (11, 34), and over 20 virus-specific MHC-I restricted peptide epitopes have been previously mapped (14, 18, 26, 53). The kinetics of viral infection have been described for both acute and chronic strains of the virus (31, 55), and LCMV-specific CD8⁺ T cells are required to clear acute infection as well as to protect from chronic or lethal challenge (1, 17, 31, 32, 41).

In these studies, we found that vaccination with H₂O₂-inactivated whole-virus LCMV vaccine (H₂O₂-LCMV) stimulated a distinct subset of the 20 different MHC-I restricted CD8⁺ T cell responses observed during acute or chronic LCMV infection. The vaccine-induced CD8⁺ T cell responses were highly polyfunctional, expressing a cytokine production profile associated with protective antiviral T cell immunity (8). Interestingly, these polyfunctional T cells were present at time points as early as 8 days postvaccination, whereas CD8⁺ T cells induced by acute LCMV strain Arm infection required several weeks to achieve a similar cytokine production profile. Once immunodominance was established by H₂O₂-LCMV vaccination, it did not change following

Received 15 August 2012 Accepted 3 October 2012

Published ahead of print 10 October 2012

Address correspondence to Mark K. Slifka, slifkam@ohsu.edu.

Copyright © 2012, American Society for Microbiology. All Rights Reserved.

doi:10.1128/JVI.02178-12

booster vaccination or subsequent viral infection. This is in contrast to the gradually shifting immunodominance pattern observed following acute LCMV Arm infection. The T cell responses to individual peptide epitopes in animals that were vaccinated with H₂O₂-LCMV prior to challenge with live virus were robust, and they constituted 25 to 50% of the total CD8⁺ T cell compartment during the memory phase of the immune response. Most importantly, animals vaccinated with H₂O₂-LCMV were protected from challenge with chronic LCMV clone 13 in a CD8⁺ T cell-dependent manner. These results indicate that the CD8⁺ T cell response elicited by H₂O₂-inactivated LCMV vaccination differs sharply from the response to LCMV infection while providing effective CD8⁺ T cell-mediated protection against chronic infection.

MATERIALS AND METHODS

Animals. Female C57BL/6, SCID, and Rag2^{-/-} mice were purchased from Jackson Laboratory (Bar Harbor, ME) and used at 6 to 20 weeks of age. All mice were housed at the Vaccine and Gene Therapy Institute according to standards of the Institutional Animal Care and Use Committee (IACUC). The Oregon Health & Sciences University (OHSU) IACUC approved all animal use protocols.

Virus and vaccines. LCMV Arm and LCMV clone 13 were grown on BHK-21 cells (ATCC) at a multiplicity of infection (MOI) of 0.1. Virus was harvested after 48 h and purified from tissue culture supernatant via ultracentrifugation at 80,000 × *g* at 4°C for 3 h over a 25% glycerol cushion. Pelleted virus was dialyzed against 3 exchanges of phosphate-buffered saline (PBS) (4 to 12 h at 4°C per exchange) to remove glycerol and soluble proteins or contaminants. Purified virus to be used for vaccination was inactivated by treatment with 3% H₂O₂ for 4 h at room temperature. Heat-inactivated LCMV was prepared by warming the virus to 56°C for 30 min. Formaldehyde-inactivated LCMV was prepared by treating the virus with 1% formaldehyde for 1 h at 4°C. Inactivated virus was then dialyzed against 3 exchanges of PBS (4 to 12 h at 4°C per exchange) to remove H₂O₂ or formaldehyde. Inactivation was confirmed by Vero cell plaque assay, coculture experiments on BHK cells, and injection into highly susceptible SCID or Rag2^{-/-} mice, followed by serum plaque assay to test for viremia at 7, 14, and 21 days after injection. Vaccine was formulated using 50 μg H₂O₂-inactivated LCMV Arm and 5 μg monophosphoryl lipid A (MPL) (InvivoGen, San Diego, CA) in 100 μl RPMI medium. Purified LCMV contained ~10⁷ PFU/μg or approximately 5 × 10⁸ PFU equivalents per dose of vaccine.

For acute infections, 2 × 10⁵ PFU LCMV Arm was administered intraperitoneally. In chronic LCMV challenge experiments, animals were injected intravenously with 2 × 10⁶ PFU LCMV clone 13 and viremia was measured weekly for 35 days. H₂O₂-LCMV vaccinations were performed by subcutaneous injection at the base of the tail.

Peptides. The peptides used in these experiments were a subset of the H-2^b-restricted epitopes to the three major LCMV proteins, nucleoprotein (NP), glycoprotein (GP), and RNA polymerase (L protein), identified previously (14, 18, 26, 53). High-performance liquid chromatography (HPLC)-purified (>95% pure) peptides were purchased from Sigma (St. Louis, MO) and GenScript (Piscataway, NJ). These peptides were reconstituted in dimethyl sulfoxide (DMSO) at a concentration of 4 × 10⁻² M. The peptides (with sequences and optimal concentrations used for T cell stimulation in parentheses) included the following: LCMV NP165-175 (SLLLNQFGTM, 10⁻⁴ M), NP205-212 (YTVKYPNL, 10⁻⁶ M), NP238-248 (SGYNFSLGAAV, 10⁻⁶ M), NP396-404 (FQPQNGQFI, 10⁻⁶ M), GP33-41 (AVYNFATM, 10⁻⁶ M), GP61-80 (GLKGPDIYKGVYQFKSVEFD, 10⁻⁵ M), GP92-101 (CSANNSHHYI, 10⁻⁶ M), GP118-125 (ISHNFCNL, 10⁻⁶ M), GP221-228 (SQTSYQYL, 10⁻⁴ M), GP276-286 (SGVENPGGYCL, 10⁻⁶ M), GP365-372 (MGVPYCNV, 10⁻⁵ M), L156-163 (ANFKERDL, 10⁻⁴ M), L313-320 (TSTEYERL, 10⁻⁴ M), L338-346 (RQLNLDVL, 10⁻⁴ M), L349-357 (SSLIKQSKF, 10⁻⁵ M), L455-463

(FMKIGAHPI, 10⁻⁴ M), L663-671 (VVYKLLRFL, 10⁻⁶ M), L775-782 (SSFNNGTL, 10⁻⁴ M), L1428-1435 (NSIQRRRL, 10⁻⁴ M), and L2062-2069 (RSIDFERV, 10⁻⁶ M). In preliminary experiments, we were unable to reproducibly identify CD8⁺ T cell responses to peptides GP44-52, L689-697, L743-751, L1189-1196, L1302-1310, L1369-1377, and L1878-1885.

Peptide stimulation and cytokine staining. Intracellular cytokine staining (ICCS) was performed as previously described (39). Briefly, splenocytes were stimulated with peptide for 6 h at 37°C and 6% CO₂ in RPMI medium containing 10% fetal bovine serum (FBS) in the presence of 2 μg/ml brefeldin A, followed by staining for CD8α peridinin chlorophyll protein (PerCP)-Cy5.5 (clone 53-6.7; eBioscience, San Diego, CA) and Aqua LIVE/DEAD fixable dead-cell stain (Invitrogen, Carlsbad, CA) overnight at 4°C. The following day, cells were fixed, permeabilized, and stained for anti-IFN-γ-fluorescein isothiocyanate (FITC) (clone XMG1.2, Invitrogen, Carlsbad, CA), anti-tumor necrosis factor alpha-phycoerythrin (anti-TNF-α-PE) (clone MP6-XT22; eBioscience), and anti-interleukin 2-allophycocyanin (anti-IL-2-APC) (clone JE S6-5H4; BioLegend, San Diego, CA). MHC-I tetramer staining was performed using anti-CD8α-PerCP-Cy5.5, anti-CD11a-PE (clone 2D7; BioLegend), and D^b-restricted tetramers, GP33-41-APC or NP396-404-APC, and a K^b-restricted tetramer, GP34-41-APC (National Institutes of Health Tetramer Core Facility, Atlanta, GA) for 1 h at 4°C, followed by washing and fixation. ICCS and tetramer samples were acquired using an LSR-2 (BD Biosciences, San Jose, CA) flow cytometer and analyzed using FlowJo software (Treestar, Ashland, OR). The forward-scatter (FSC) area versus FSC height gate was used as a singlet gate to remove clumped cells from analysis. Samples were gated on Aqua-negative cells to include cells that were viable at the conclusion of the assay. Lymphocyte gating was performed based on FSC and side scatter (SSC) characteristics, and CD8⁺ gates were then applied before the percentage of cytokine-positive T cells was determined.

Serum samples and plaque assays. Whole blood was collected from a tail vein and allowed to coagulate at room temperature for 2 h. The blood was centrifuged at 16,000 relative centrifugal force (RCF) for 1 min, and serum was collected and transferred to a new tube. The serum was again centrifuged at 16,000 RCF for 1 min, and serum was collected and stored at -80°C until plaque assays were performed.

Plaque assays were performed as described previously (2). Plaque assay plates were seeded using 3 × 10⁵ Vero cells per well in 6-well plates. Plates were incubated overnight, medium was discarded, and the wells were overlaid with 200 μl of 10-fold serially diluted serum and incubated for 1 h at 37°C and 6% CO₂. Wells were then overlaid with 3 ml 0.5% agarose in Eagle minimal essential medium (EMEM) supplemented with 2.5% FBS, antibiotics, and 2 mM glutamine and incubated at 37°C and 6% CO₂ for 5 days. Wells were then overlaid with 1 ml 1% agarose containing 0.1 to 0.2% neutral red (Sigma-Aldrich, St. Louis, MO), and plaques were counted 12 to 18 h later.

CD8⁺ T cell depletion. CD8⁺ T cell depletion was performed as previously described (46). Animals were given 100 μg purified anti-CD8α monoclonal antibody, 2.43 (BioXCell, West Lebanon, NH), administered intraperitoneally on days -2, 0, +2, and +4 relative to LCMV clone 13 challenge.

RESULTS

H₂O₂ inactivation of LCMV. When 3% H₂O₂ is used to inactivate purified LCMV, viable infectious virus declines with a <13-s half-life, and it is typical to achieve greater than a millionfold reduction in infectious virus titer within 2 h (reference 4 and data not shown). In these studies, LCMV was inactivated for an additional 2 h after loss of detectable infectivity (i.e., 4 h total), and complete LCMV inactivation was confirmed by directly performing plaque assays or by coculturing up to 200 μg inactivated material (i.e., >10⁹ PFU) on BHK cells followed by plaque assay. As an additional test for live virus, RAG2^{-/-} animals were injected intraperi-

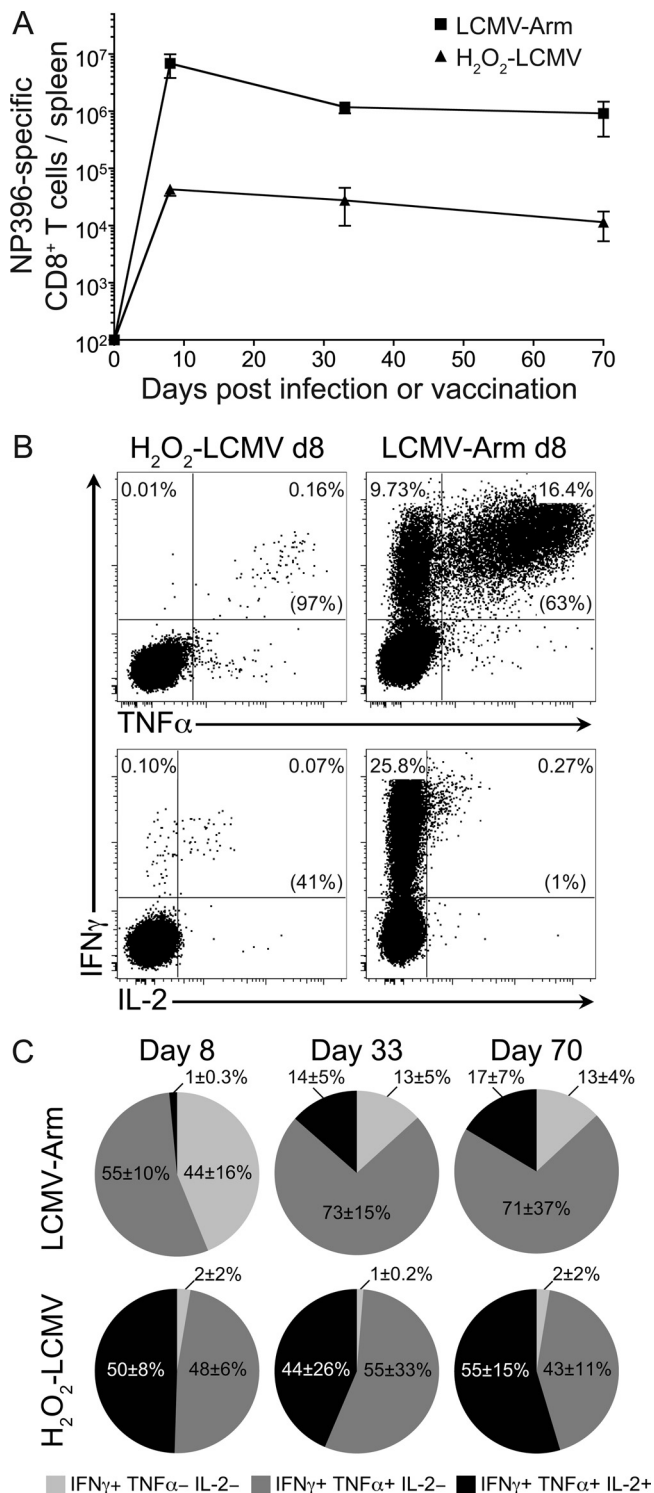


FIG 1 H₂O₂-LCMV vaccination induces long-lived polyfunctional CD8⁺ T cell immunity. C57BL/6 mice were vaccinated with 50 μg H₂O₂-LCMV formulated with 5 μg MPL or infected with 2 × 10⁵ PFU LCMV Arm. CD8⁺ T cells were stimulated directly *ex vivo* with the immunodominant LCMV peptide, NP396, and antiviral T cell responses were analyzed by ICCS. (A) The total number of IFN-γ-producing CD8⁺ T cells per spleen was calculated at days 8, 33, and 70 after H₂O₂-LCMV vaccination or LCMV Arm infection. (B) Representative cytokine production profiles at 8 days following vaccination or infection were determined directly *ex vivo*. Data in parentheses are percentages of IFN-γ-positive T cells that coexpressed either TNF-α or IL-2. (C) Average

toneally with up to 200 μg of inactivated material and viremia was subsequently measured using plaque assay. Coculture and RAG2^{-/-} mouse infection assays represent independent tests that are each capable of detecting 1 or 2 infectious virus particles per sample, and they confirmed that the H₂O₂-LCMV vaccine material used in these studies was devoid of detectable live virus.

H₂O₂-LCMV vaccination stimulates a long-lasting and polyfunctional NP396-specific CD8⁺ T cell response. Primary infection of C57BL/6 mice with LCMV Arm induces a CD8⁺ T cell response that peaks in magnitude at about 7 to 8 days postinfection. This response then declines 10- to 20-fold to become a stable memory response between 1 and 2 months after infection (33, 56). To compare the levels of T cell memory generated by our H₂O₂-LCMV vaccine to the responses induced by LCMV Arm infection, we measured the CD8⁺ T cell responses to the immunodominant epitope, LCMV NP396, from 8 to 70 days after infection or vaccination (Fig. 1A). At day 8, the average number of NP396-specific CD8⁺ T cells per spleen was about 150-fold lower in the H₂O₂-LCMV-vaccinated mice than in the LCMV Arm-infected mice. However, the levels of virus-specific CD8⁺ T cells in vaccinated animals declined only 30 to 40% between day 8 and day 35 after vaccination, whereas T cell responses in the LCMV Arm-infected animals declined by 80 to 90% during the same period. By 70 days after vaccination or infection, there was about an 80-fold difference in the total number of NP396-specific CD8⁺ T cells per spleen between the two experimental groups. Although H₂O₂-LCMV vaccination induces an NP396-specific T cell response that was lower in magnitude than the response to LCMV Arm infection, both forms of T cell memory appeared relatively stable over the course of the observation.

Polyfunctional T cells (i.e., T cells capable of producing multiple cytokines following peptide stimulation) have been associated with more effective control of chronic viral infections, such as infections with cytomegalovirus (CMV) and HIV (8, 42, 49). The CD8⁺ T cell response to LCMV Arm infection also becomes more polyfunctional over the course of weeks or months as it transitions from an effector to a memory response (47, 57, 59). Interestingly, we found that H₂O₂-LCMV vaccine-induced CD8⁺ T cells were capable of producing multiple cytokines as early as 8 days after vaccination (Fig. 1B and C). On average, 98% of IFN-γ⁺ NP396-specific CD8⁺ T cells coexpressed TNF-α in response to direct *ex vivo* peptide stimulation at day 8 postvaccination. In contrast, only 55% of NP396-specific CD8⁺ T cells at day 8 postinfection produced both IFN-γ and TNF-α. Similar to the case with BALB/c mice (4), the disparity in IL-2 production between virus-specific CD8⁺ T cells from H₂O₂-LCMV-vaccinated C57BL/6 mice and LCMV Arm-infected mice at 8 days after infection was even greater. In this case, 50% of the vaccine-induced IFN-γ⁺ CD8⁺ T cells were able to produce IL-2 following NP396 peptide stimulation, whereas only 1% of the IFN-γ⁺ CD8⁺ T cells elicited pep-

cytokine profiles following infection or vaccination were determined at 8, 33, or 70 days after infection or vaccination. The three cytokine production profiles shown are based on single positive (IFN-γ⁺ only), double positive (IFN-γ⁺ and TNF-α⁺), and triple positive (IFN-γ⁺, TNF-α⁺, and IL-2⁺) events. Production of other cytokines in other combinations did not exceed background values. Data represent the averages ± SDs from 3 or 4 mice per group at each time point from 2 independent experiments. Note that in some cases, the SD error bars are smaller than the size of the symbol used to represent the individual data point.

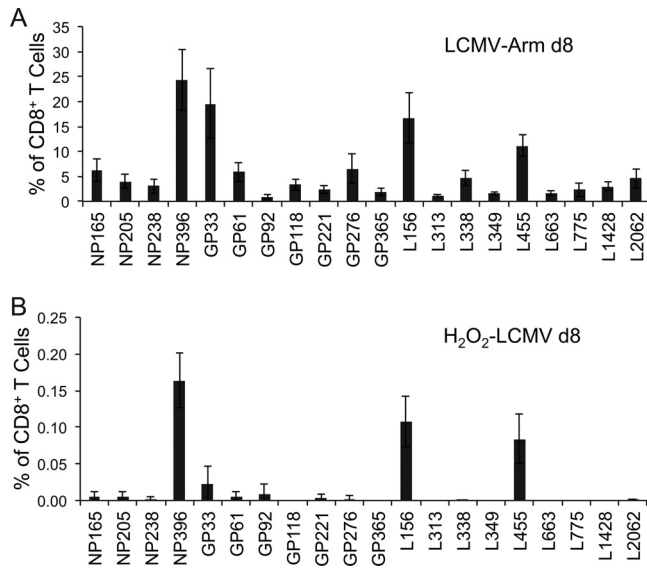


FIG 2 CD8⁺ T cell immunodominance profiles differ following acute LCMV Arm infection or H₂O₂-LCMV vaccination. C57BL/6 mice were infected with LCMV Arm or vaccinated with H₂O₂-LCMV. Eight days later, T cell cultures were stimulated directly *ex vivo* with one of 20 individual H-2^b-restricted LCMV peptides, and IFN- γ cytokine expression was determined using ICCS. Immunodominance profiles following primary LCMV Arm infection (A) or H₂O₂-LCMV vaccination (B) were determined based on the percentage of CD8⁺ T cells expressing IFN- γ after background subtraction of medium-only controls. Graphs show the averages \pm SDs of 3 or 4 mice per group from 2 independent experiments.

tide-specific IL-2 production in response to LCMV Arm infection. CD8⁺ T cells from LCMV Arm-infected animals had an evolving cytokine profile that became more polyfunctional as the T cells progressed from the effector to the memory phase of the immune response. By 70 days postinfection, the percentage of NP396-specific T cells that were capable of producing IFN- γ , TNF- α , and IL-2 in response to peptide stimulation increased from 1% to 17%. Even with this improvement in function, the virus-specific T cells from LCMV Arm-infected animals did not achieve the same percentage of polyfunctional CD8⁺ T cells as the virus-specific T cells from H₂O₂-LCMV-vaccinated animals. H₂O₂-LCMV vaccination consistently induced a higher proportion of IFN- γ ⁺ TNF- α ⁺ IL-2⁺ CD8⁺ T cells, with 44 to 55% of the NP396-specific population expressing these three cytokines at each time point examined. These data indicate that the H₂O₂-LCMV vaccine strategy is capable of inducing CD8⁺ T cell responses that are durable and have a higher proportion of polyfunctional T cells than the immune responses elicited by acute LCMV Arm infection.

Immunodominance following acute LCMV Arm infection or vaccination with inactivated LCMV. The CD8⁺ T cell response to LCMV is well characterized and provides the opportunity to investigate potential differences in the immunodominance hierarchies between H₂O₂-LCMV-vaccinated animals and LCMV Arm-infected animals (Fig. 2). We selected a panel of the 20 most immunogenic LCMV peptides, consisting of 4 nucleoprotein epitopes (NP165, NP205, NP238, and NP396), 7 glycoprotein epitopes (GP33, GP61, GP92, GP118, GP221, GP276, and GP365), and 9 polymerase epitopes (L156, L313, L338, L349, L455, L663, L775, L1428, and L2062). Following acute LCMV

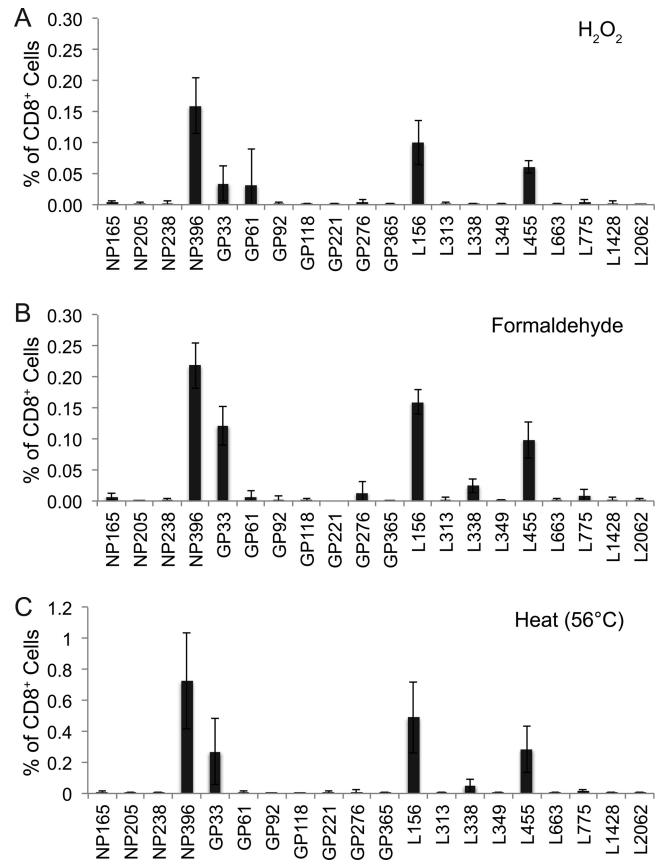


FIG 3 CD8⁺ T cell immunodominance profiles are similar following vaccination with LCMV inactivated by H₂O₂, formaldehyde, and heat. C57BL/6 mice were vaccinated with 50 μ g purified LCMV inactivated with H₂O₂ (A), formaldehyde (B), or heat (56°C) (C), each formulated with 5 μ g MPL. Immunodominance profiles were determined 8 days following vaccination by direct *ex vivo* stimulation of splenocytes with the panel of 20 H-2^b-restricted LCMV peptides. Graphs show the averages \pm SDs of 4 mice per group from 2 independent experiments.

Arm infection (Fig. 2A), T cell responses to NP396, GP33, and L156 were codominant, and intermediate responses (consisting of $\geq 5\%$ of the CD8⁺ T cell population) were observed with L455, NP165, GP61, and GP276 peptide stimulation. Reproducible, albeit low-frequency, T cell responses were also observed after stimulation with 13 other LCMV peptides (Fig. 2A). In sharp contrast to live viral infection, H₂O₂-LCMV vaccination elicited an immunodominance pattern that was restricted to 3 main peptide epitopes, NP396, L156, and L455 (Fig. 2B). A weak CD8⁺ T cell response to GP33 was sometimes observed, though the average GP33 response was less than 2-fold over background and was not detected in all vaccinated animals. A similar immunodominance pattern was observed if mice were vaccinated with LCMV inactivated with H₂O₂ (Fig. 3A), formaldehyde (Fig. 3B), or heat (56°C) (Fig. 3C), suggesting that the immunodominance pattern observed following H₂O₂-LCMV vaccination was not necessarily restricted to H₂O₂ inactivation, since similar results were obtained with other inactivation approaches as well. Interestingly, although formaldehyde-based virus inactivation was similar to that observed with H₂O₂-based virus inactivation, heat inactivation resulted in modestly higher CD8⁺ T cell responses, which may have

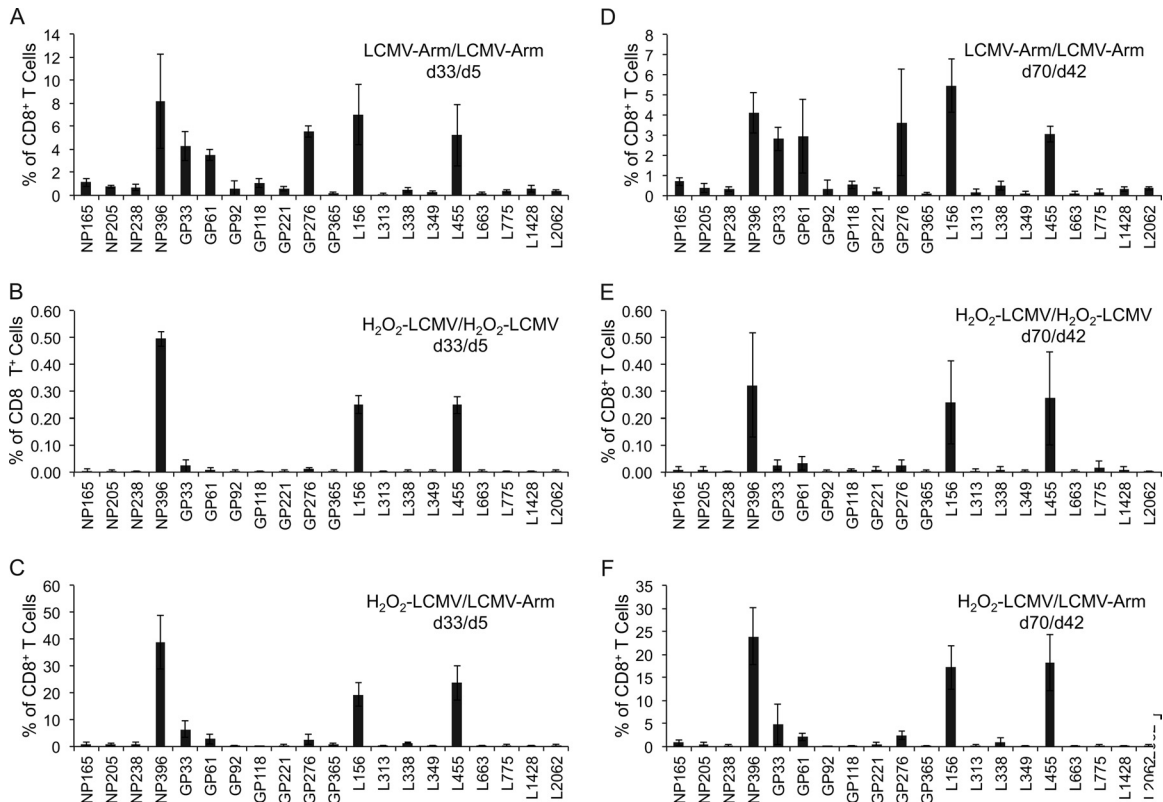


FIG 4 H₂O₂-LCMV-vaccinated mice maintain stable CD8⁺ T cell immunodominance patterns following subsequent infection or booster vaccination. C57BL/6 mice underwent primary infection with 2×10^5 PFU LCMV Arm or vaccination with H₂O₂-LCMV and 28 days later received a secondary live LCMV challenge or booster H₂O₂-LCMV vaccination. Combinations included LCMV Arm infection followed by LCMV Arm challenge (A and D), H₂O₂-LCMV vaccination followed by H₂O₂-LCMV boost (B and E), and H₂O₂-LCMV vaccination followed by LCMV Arm challenge (C and F). Immunodominance profiles were determined by stimulating T cells with a panel of 20 LCMV peptides followed by IFN- γ ICCS at day 5 (A to C) or day 42 (D to F) postchallenge or after booster vaccination. The data represent the averages \pm SDs of 3 or 4 mice per group from 2 independent experiments.

been due to aggregation since heat-inactivated virus formed readily visible clumps (data not shown) and protein aggregation is known to increase CD8⁺ T cell priming *in vivo* (23, 48).

Although the overall magnitude of T cell responses elicited by primary H₂O₂-LCMV vaccination was low, direct *ex vivo* peptide stimulation allowed detection of T cell responses as low as 0.04% of the CD8⁺ T cell population. To determine if booster vaccination would increase T cell responses or make it possible to detect rare T cell populations specific to more subdominant epitopes, we conducted a series of prime-boost experiments (Fig. 4). In these studies, animals were vaccinated with H₂O₂-LCMV or infected with LCMV Arm at day 0. H₂O₂-LCMV-vaccinated animals were then boosted by H₂O₂-LCMV vaccination or LCMV Arm infection 28 days later. For comparison, LCMV Arm-infected animals were boosted with a second LCMV Arm infection at day 28 after primary infection. The CD8⁺ T cell responses were then analyzed at 5 days (Fig. 4A to C) or 42 days (Fig. 4D to F) after secondary vaccination or infection. When animals were infected at day 0 and challenged at day 28 with LCMV Arm, we observed several changes in immunodominance, with GP276 emerging as a codominant epitope along with NP396, GP33, GP61, L156, and L455 (Fig. 4A). Increased immunodominance of GP276 during secondary LCMV infection has been noted previously (51). By day 42, CD8⁺ T cell responses to the other 14 individual peptides each represented less than 1% of the CD8⁺ T cell response. When

H₂O₂-LCMV-vaccinated animals were boosted with H₂O₂-LCMV at day 28, the result was strikingly different, with no evolution of the immunodominance profile. There was an average 3-fold increase in the magnitude of the LCMV-specific CD8⁺ T cell responses following booster vaccination, but there was no change in immunodominance hierarchy between the responses noted after primary H₂O₂-LCMV vaccination (Fig. 2B), 5 days after secondary H₂O₂-LCMV vaccination (Fig. 4B), or 42 days after secondary H₂O₂-LCMV vaccination (Fig. 4E). This phenomenon of “fixed” immunodominance was also observed when H₂O₂-LCMV-vaccinated animals were boosted with LCMV Arm. These animals displayed essentially the same immunodominance profile as the other vaccinated animals, generating a dominant response to NP396 and two subdominant responses to L156 and L455 (Fig. 4C and F). However, the T cell responses elicited against these 3 immunodominant peptide epitopes expanded dramatically following LCMV Arm challenge. The response to NP396 alone comprised nearly 40% of the host’s total CD8⁺ T cell compartment at day 5 after challenge (Fig. 4C) and remained at 24% of the total CD8⁺ T cell compartment at day 42 following challenge (Fig. 4F). These data indicate that while the H₂O₂-LCMV vaccine-induced CD8⁺ T cell responses constitute a small percentage of the total CD8⁺ T cell repertoire after primary vaccination, these responses exhibit remarkably stable immunodominance patterns and are capable of rapidly expanding to high frequencies that re-

main at elevated levels following resolution of acute viral infection.

H₂O₂-LCMV vaccination provides protection against chronic LCMV clone 13 challenge. LCMV clone 13 infection causes chronic infection as well as predictable T cell dysfunction, both of which are preventable if infected animals have a preexisting LCMV-specific CD8⁺ T cell response (29, 35, 43, 44, 46, 50). As expected, naïve C57BL/6 mice became chronically infected with LCMV clone 13, with viremia lasting for at least 35 days (Fig. 5A). LCMV Arm-immune animals were protected from chronic LCMV clone 13 challenge and showed no detectable viremia at any time point examined. Similar to a prior study using BALB/c mice (4), we next determined whether H₂O₂-LCMV vaccination was protective against chronic LCMV challenge of C57BL/6 mice. Animals were vaccinated with H₂O₂-LCMV at either 8 days or 28 days prior to challenge with LCMV clone 13. All of the animals vaccinated 8 days prior to challenge were protected against LCMV clone 13 viremia (<50 PFU/ml). Animals vaccinated 28 days prior to challenge demonstrated >100-fold reduction in viremia compared to that in naïve animals, with 5/7 (71%) being fully protected against viremia at 7 days postchallenge and 100% of the vaccinated animals demonstrating antiviral protection by 14 days postchallenge. This degree of protection against LCMV clone 13 is similar to that achieved in previous studies using live recombinant *Listeria monocytogenes* expressing the LCMV nucleoprotein (46). The mechanism of protection afforded by H₂O₂-LCMV vaccination has not been formally determined, and for this reason, we examined the role of CD8⁺ T cells in mediating vaccine-induced protection against LCMV clone 13 challenge. An experiment was performed in which a group of H₂O₂-LCMV-vaccinated animals were depleted of CD8⁺ T cells prior to challenge with LCMV clone 13 (Fig. 5B). Similar to the results shown in Fig. 5A, animals that had received H₂O₂-LCMV 8 days prior to LCMV clone 13 challenge showed no detectable viremia at 7 days postchallenge. In contrast, if CD8⁺ T cells were depleted at the time of infection, then LCMV clone 13 viremia was indistinguishable from that in the naïve controls. Together, these data show that the CD8⁺ T cell responses generated by H₂O₂-LCMV vaccination are required for protection against chronic LCMV infection.

Chronic infection may alter immunodominance (52, 55, 64), and we examined this issue by measuring CD8⁺ T cell responses at 35 days after LCMV clone 13 challenge using our panel of 20 LCMV peptides. Functional (i.e., IFN- γ ⁺) peptide-specific CD8⁺ T cell responses are presented as a percentage of the total CD8⁺ T cell compartment to illustrate differences in the magnitude of T cell responses between the vaccinated and control groups (Fig. 5C, E, G, and I), or they are presented as the percentage of the LCMV-specific CD8⁺ T cell response to more clearly illustrate differences in immunodominance patterns (Fig. 5D, F, H, and J). In naïve animals, CD8⁺ T cell responses to NP396 undergo depletion after LCMV clone 13 infection (55, 64). Likewise, we found that NP396 and L455 underwent deletion or exhaustion and responses to GP33 became dysfunctional, with fewer T cells able to produce IFN- γ in response to peptide stimulation than would be expected based on peptide-MHC tetramer staining performed in parallel (Fig. 5C and data not shown). Interestingly, GP276 and L156 emerged as the immunodominant T cell epitopes following LCMV clone 13 infection of unvaccinated CD57BL/6 mice (Fig. 5D). Animals infected with LCMV Arm 28 days prior to challenge (Fig. 5E) suffered no obvious T cell dysfunction and had immu-

nodominance profiles similar to those of animals examined 6 weeks following LCMV Arm challenge (Fig. 4D). Animals challenged either 8 days (Fig. 5G) or 28 days (Fig. 5I) after H₂O₂-LCMV vaccination had immunodominance profiles that remained similar to those of animals receiving H₂O₂-LCMV vaccination alone (Fig. 4). In addition, the vaccinated animals maintained large memory T cell responses to the 3 major epitopes, NP396, L156, and L455, following LCMV clone 13 challenge. Indeed, the average T cell response to the immunodominant NP396 epitope in the group vaccinated 8 days prior to LCMV clone 13 challenge was maintained at 41% of the total CD8⁺ T cell compartment at day 35 postchallenge. Vaccinated animals did not display CD8⁺ T cell dysfunction, and the subdominant responses to the GP33 epitope were equivalent when measured by ICCS or peptide-MHC tetramer (data not shown). The preferential loss of NP396 and L455 CD8⁺ T cell responses in the naïve animals infected with LCMV clone 13 (Fig. 5D) resulted in substantial skewing of normal immunodominance in comparison with the animals that were LCMV immune prior to challenge (Fig. 5F). In sharp contrast, animals that were vaccinated with H₂O₂-LCMV prior to LCMV clone 13 challenge showed immunodominance patterns that were similar to each other (Fig. 5H and I) and remained unaltered from the immunodominance profile observed following H₂O₂-LCMV vaccination alone (Fig. 2B).

DISCUSSION

In these experiments, we generated a H₂O₂-inactivated whole-virus vaccine against LCMV and tested it in terms of CD8⁺ T cell immunogenicity and protective efficacy in C57BL/6 mice. Our results demonstrate that vaccination with H₂O₂-LCMV generated an LCMV-specific memory CD8⁺ T cell response that persisted for at least 10 weeks after a single vaccination. The vaccine-induced CD8⁺ T cells demonstrated a highly polyfunctional cytokine profile, with close to 50% of the responding T cells capable of producing at least 3 cytokines in response to peptide stimulation (IFN- γ ⁺, TNF- α ⁺, and IL-2⁺) as early as 8 days after vaccination. Our results show that H₂O₂-LCMV vaccination induced a small but highly reproducible subset of the 20 epitope-specific CD8⁺ T cell responses observed following LCMV Arm infection. Once established, the vaccine-induced immunodominance profile did not change over time or following subsequent LCMV infection, and this was in contrast to the shifting immunodominance profiles observed after acute or chronic LCMV infection. The H₂O₂-inactivated LCMV vaccine also protected animals against chronic LCMV clone 13 challenge in a CD8⁺ T cell-dependent manner. These results indicate that the H₂O₂-inactivated vaccine platform is capable of generating protective T cell immunity.

This study is an extension of prior work performed with BALB/c mice demonstrating that H₂O₂-inactivated vaccines are capable of eliciting highly effective antiviral neutralizing antibody responses in addition to antigen-specific CD8⁺ T cell responses (4). The goal of this study was to examine LCMV-specific CD8⁺ T cell immunodominance and how it might be altered by vaccination with an inactivated whole-virus vaccine. Studies on LCMV-specific immunodominance are difficult to perform with BALB/c mice because >90% of the antiviral CD8⁺ T cell response is directed against a single immunodominant peptide epitope, NP118-126. In contrast, by examining H₂O₂-LCMV vaccination of C57BL/6 mice, we were able to demonstrate vaccine-induced CD8⁺ T cell responses in mice with a different MHC haplotype

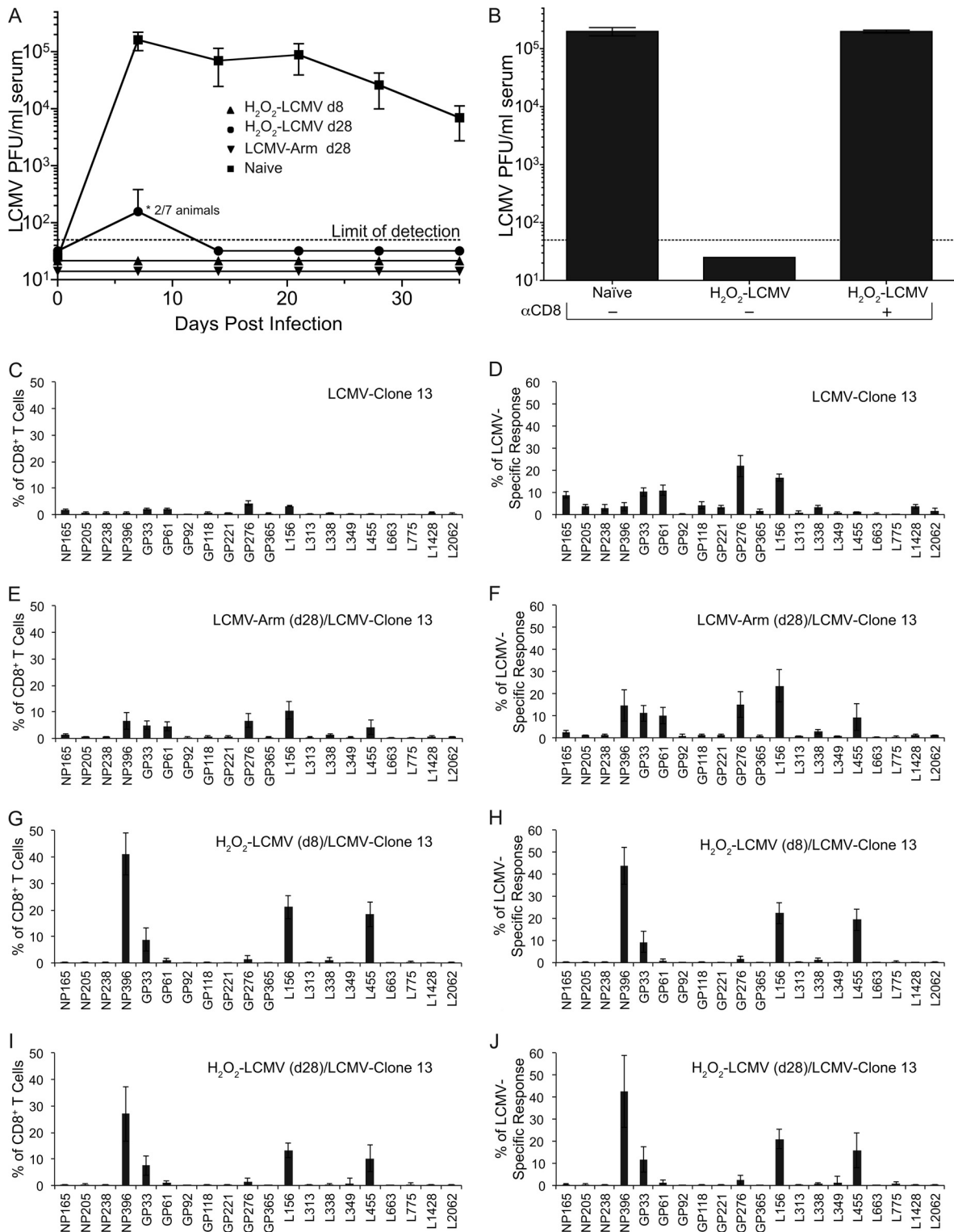


FIG 5 H₂O₂-LCMV vaccination protects mice against chronic LCMV clone 13 challenge in a CD8⁺ T cell-dependent manner. C57BL/6 mice were challenged with 2×10^6 PFU LCMV clone 13 at 8 days or 28 days following H₂O₂-LCMV vaccination or at 28 days following LCMV Arm infection. Serum viremia was determined by plaque assay at weekly intervals (A). To determine if vaccine-induced protection from challenge was CD8⁺ T cell mediated, a group of animals were vaccinated with H₂O₂-LCMV followed by CD8⁺ T cell depletion and LCMV clone 13 challenge (B). CD8⁺ T cell immunodominance was determined at day 35 following LCMV clone 13 challenge by stimulating T cells with the panel of 20 individual LCMV peptides directly *ex vivo* followed by ICCS (C to J). Prior to LCMV clone 13 challenge, the animals were either naive (C and D), infected with LCMV Arm (E and F), or vaccinated with H₂O₂-LCMV (G to J). LCMV clone 13 challenge occurred 8 days (G and H) or 28 days (E, F, I, and J) following infection or vaccination. Immunodominance profiles are displayed as the percentage of CD8⁺ T cells producing IFN- γ in response to each peptide (C, E, G, and I) or as the percentage of the total LCMV-specific response (D, F, H, and J). Graphs show the averages \pm SDs of 3 to 7 mice per group from 2 independent experiments.

and study antiviral immunity against up to 20 different peptide epitopes. Using the C57BL/6 model system, we discovered significant and somewhat surprising differences in immunodominance patterns following vaccination versus acute or chronic LCMV infection. In addition, this study provided the first formal analysis of the mechanism of H₂O₂-LCMV vaccine-mediated protection by demonstrating that vaccine-induced CD8⁺ T cells were required for protective immunity against chronic LCMV infection (Fig. 5).

Different immunodominance patterns emerged in C57BL/6 mice and depended on whether viral antigen was presented in the context of acute infection, chronic infection, or vaccination. Acute LCMV Arm infection generated a CD8⁺ T cell response against at least 20 peptide epitopes (26) (Fig. 2A). This response to infection had an evolving immunodominance profile as the T cells progressed from the effector phase to the memory phase of T cell maturation (38), and it changed further in response to LCMV Arm or LCMV clone 13 rechallenge (Fig. 4 and 5). Of the 20 peptides examined, the most immunodominant epitopes following primary LCMV Arm infection were NP396, GP33 (containing both GP33 and GP34 epitopes), L156, and L445. This array of immunodominant epitopes expanded during reinfection with LCMV Arm or LCMV clone 13 to include NP396, GP33, GP61, GP276, L156, and L455. During the diminished antiviral T cell response elicited during primary LCMV clone 13 infection, GP276 and L156 were the immunodominant epitopes, and the responses to previously codominant epitopes (e.g., NP396, GP33, GP61, and L455) were reduced, deleted, or dysfunctional. Interestingly, the immunodominance pattern following H₂O₂-LCMV vaccination was vastly different from the patterns observed during either acute or chronic LCMV infection. After primary vaccination (Fig. 2) or vaccination followed by LCMV challenge (Fig. 4 and 5), the most immunodominant T cell responses remained directed against only three epitopes: NP396, L156, and L455. It will be important to determine if these represent three independent peptide-specific T cell responses or if there may be cross-reactivity between these epitopes, similar to what has been observed in the influenza model system (7).

Arenavirus virions contain NP, GP, and L proteins (10), indicating that differences in immunodominance observed in H₂O₂-LCMV-immunized animals were not simply due to one or more of the viral proteins being absent from the purified whole-virus vaccine formulation. In the case of LCMV-GP, vaccine-induced T cell responses were typically below the level of detection, which is in contrast to T cell responses elicited following live LCMV infection (Fig. 2). The vaccine-induced T cell responses to GP epitopes were not boosted by secondary vaccination or virus challenge (Fig. 4 and 5), indicating that the failure to identify GP-specific CD8⁺ T cell responses during primary vaccination was unlikely to be due to a low threshold of detection, since booster vaccination or infection readily augmented vaccine-induced T cell responses to NP396, L156, and L455. It seems unlikely that different immunodominance patterns are due to preferential oxidative damage to the LCMV surface glycoprotein, since formaldehyde-based inactivation and heat inactivation also result in skewed immunodominance profiles (Fig. 3). Oxidation by H₂O₂ is believed to inactivate microbes by multiple mechanisms, including disruption of lipid membrane bilayers, oxidation of protein backbones and amino acid side chains, and oxidation of nucleosides (6, 16). Damage to nucleic acids, including the induction of single-strand and double-strand breaks in genomic RNA or DNA, is a likely mechanism

of irreversible microbial inactivation (60, 63) and is expected to result in similar oxidation of internal viral proteins, including the LCMV nucleoprotein and L protein. We also observed peptide-specific differences in CD8⁺ T cell responses to LCMV epitopes within the same protein. For instance, NP396 was immunodominant after H₂O₂-LCMV vaccination, but detectable T cell responses to other NP epitopes, including NP165, NP205, and NP238, were not induced by H₂O₂-inactivated LCMV. Similar skewing of immunogenicity was also observed in L protein epitopes in which only 2 (L156 and L455) of the 9 potential L epitopes were elicited by vaccination (Fig. 2). These intraprotein differences in peptide immunogenicity suggest that other mechanisms besides protein abundance may be responsible for the unique LCMV-specific CD8⁺ T cell immunodominance patterns observed following vaccination with H₂O₂-LCMV.

Peptide affinity for MHC-I plays an important role in determining immunogenicity, although high-affinity peptides that are above a certain threshold are not necessarily more likely to produce more immunodominant CD8⁺ T cell responses (27). Likewise, when we compared immunodominance patterns (Fig. 2, 4, and 5) with peptide affinity for MHC-I (26), we found no correlation with the hierarchy of the immunodominance profiles, which varied considerably depending on whether animals had been vaccinated or if they underwent acute or chronic LCMV infection (data not shown). The skewed immunodominance profile of virus-specific CD8⁺ T cells after H₂O₂-LCMV vaccination suggests that some antigenic determinants present in the virus are more capable of cross-priming CD8⁺ T cell responses than others. Transporter associated with antigen processing (TAP)-dependent as well as TAP-independent antigen processing pathways play a role in direct presentation as well as cross-presentation of antigen (37, 40). Interestingly, it has been observed that NP396 processing can occur via a TAP-independent pathway, whereas GP33 processing appears to occur via a TAP-dependent mechanism (21, 45). This suggests that NP396 could be more immunodominant following H₂O₂-LCMV vaccination because it is able to be cross-presented via a TAP-independent mechanism. This distinction may be less important to the development of immunodominance during LCMV infection because direct antigen presentation through the classical MHC-I pathway is likely to dominate the antiviral T cell response. Elucidating the role of TAP-dependent and TAP-independent mechanisms of antigen presentation could provide further insight into the mechanisms that govern immunodominance during immunization with inactivated whole-virus vaccines.

Utilization of antigen-presenting cells is another factor that may play a role in the different immunodominance patterns observed after LCMV Arm infection, LCMV clone 13 infection, and vaccination with H₂O₂-LCMV. There is evidence that the constellation of peptides that are presented via MHC-I can vary depending on the type of antigen-presenting cells performing the antigen presentation (12). It has been observed that dendritic cells (DC) present GP33 and NP396 peptides most efficiently following LCMV infection, whereas LCMV-infected fibroblasts are more efficient at processing and presenting GP276 following infection (12). In addition, it is believed that CD8⁺ DC are primarily responsible for cross-presentation in mice (19). This means that during LCMV Arm infection, there are likely many professional and nonprofessional types of antigen-presenting cells functioning to stimulate the CD8⁺ T cell response, whereas vaccination with

H₂O₂-LCMV may result in cross-presentation of viral antigen mainly via a narrow range of antigen-presenting cells such as CD8⁺ DC. Therefore, differences in antigen-presenting cell usage and antigen processing efficiency during H₂O₂-LCMV vaccination and LCMV Arm infection may account for some of the main differences in immunodominance observed in these studies.

Another interesting finding from these experiments was the discovery that LCMV-specific CD8⁺ T cells were maintained at surprisingly higher levels in animals that were H₂O₂-LCMV vaccinated and subsequently challenged with LCMV compared to the responses normally observed in LCMV infection or reinfection (Fig. 4 and 5). One explanation for the elevated magnitude of LCMV-specific CD8⁺ T cell memory is that a large proportion of vaccine-induced CD8⁺ T cells were capable of producing IL-2 following exposure to viral peptide antigen (Fig. 1). Autocrine IL-2 signaling may be critical to the secondary expansion of CD8⁺ T cell populations following rechallenge (15). Moreover, vaccination strategies such as DC vaccination do not induce substantial inflammatory responses but result in CD8⁺ T cell immunity that may be more easily restimulated upon antigenic challenge (36). The absence of a highly inflammatory microenvironment during H₂O₂-LCMV vaccination may afford vaccine-induced CD8⁺ T cells a selective advantage, enabling them to rapidly proliferate and be maintained at high concentrations during and after subsequent virus challenge.

These results provide an important proof of concept, demonstrating that an H₂O₂-inactivated whole-virus vaccine can be used to generate protective CD8⁺ T cell immunity against an arenavirus. Although there is a live attenuated vaccine available for Junin virus, the causative agent of Argentine hemorrhagic fever, there is no vaccine available for other clinically relevant arenaviruses such as Sabia, Machupo, and Lassa fever viruses. It remains to be determined if this approach to vaccine development will prove useful for combating these important diseases. However, the ability of H₂O₂-LCMV vaccination to induce protective CD8⁺ T cell responses in mice indicates that the H₂O₂ inactivation platform may be a potentially effective vaccine strategy under circumstances in which a CD8⁺ T cell response is important for protection.

ACKNOWLEDGMENTS

We thank the NIH Tetramer Core Facility for generously providing peptide-MHC tetramers.

Research reported in this publication was supported by National Institutes of Health grants T32 AI078903 (to J.M.W.), T32-CA106195 (to J.M.W.), R56 AI076506 (to M.K.S.), U01 AI082196 (to M.K.S.), and R43 AI079898 (to M.K.S.) and Oregon National Primate Research Center grant 8P51 OD011092-53 (to M.K.S.).

M.K.S. and J.M.W. conceived the project. H.P.R. and J.M.W. performed the viral culture and vaccine preparation. J.M.W. performed the animal studies, data analysis, and figure preparation. J.M.W. and M.K.S. wrote the manuscript. All authors discussed the results and reviewed the manuscript prior to submission.

OHSU and M.K.S. have a financial interest in Najit Technologies, Inc., a company that may have a commercial interest in the results of this research and technology. This potential individual and institutional conflict of interest has been reviewed and managed by OHSU. J.M.W. and H.P.R. declare no competing financial interests.

REFERENCES

- Ahmed R, Butler LD, Bhatti L. 1988. T4⁺ T helper cell function in vivo: differential requirement for induction of antiviral cytotoxic T-cell and antibody responses. *J. Virol.* 62:2102–2106.
- Ahmed R, Salmi A, Butler LD, Chiller JM, Oldstone MB. 1984. Selection of genetic variants of lymphocytic choriomeningitis virus in spleens of persistently infected mice. Role in suppression of cytotoxic T lymphocyte response and viral persistence. *J. Exp. Med.* 160:521–540.
- Amanna IJ, Messaoudi I, Slifka MK. 2008. Protective immunity following vaccination: how is it defined? *Hum. Vaccin.* 4:316–319.
- Amanna IJ, Raue HP, Slifka MK. 2012. Development of a new hydrogen peroxide-based vaccine platform. *Nat. Med.* 18:974–979.
- Annunziato D, et al. 1982. Atypical measles syndrome: pathologic and serologic findings. *Pediatrics* 70:203–209.
- Barelli S, et al. 2008. Oxidation of proteins: basic principles and perspectives for blood proteomics. *Proteomics Clin. Appl.* 2:142–157.
- Belz GT, Xie W, Doherty PC. 2001. Diversity of epitope and cytokine profiles for primary and secondary influenza A virus-specific CD8⁺ T cell responses. *J. Immunol.* 166:4627–4633.
- Betts MR, et al. 2006. HIV nonprogressors preferentially maintain highly functional HIV-specific CD8⁺ T cells. *Blood* 107:4781–4789.
- Brown F. 1993. Review of accidents caused by incomplete inactivation of viruses. *Dev. Biol. Stand.* 81:103–107.
- Buchmeier MJ, de la Torre JC, Peters CJ. 2007. Arenaviridae: the viruses and their replication. In Knipe DM, et al (ed), *Fields virology*, 5th ed., p 1792–1827. Lippincott Williams & Wilkins, Philadelphia, PA.
- Buchmeier MJ, Welsh RM, Dutko FJ, Oldstone MB. 1980. The virology and immunobiology of lymphocytic choriomeningitis virus infection. *Adv. Immunol.* 30:275–331.
- Butz EA, Bevan MJ. 1998. Differential presentation of the same MHC class I epitopes by fibroblasts and dendritic cells. *J. Immunol.* 160:2139–2144.
- Delgado MF, et al. 2009. Lack of antibody affinity maturation due to poor Toll-like receptor stimulation leads to enhanced respiratory syncytial virus disease. *Nat. Med.* 15:34–41.
- Dow C, et al. 2008. Lymphocytic choriomeningitis virus infection yields overlapping CD4⁺ and CD8⁺ T-cell responses. *J. Virol.* 82:11734–11741.
- Feau S, Arens R, Togher S, Schoenberger SP. 2011. Autocrine IL-2 is required for secondary population expansion of CD8(+) memory T cells. *Nat. Immunol.* 12:908–913.
- Finnegan M, et al. 2010. Mode of action of hydrogen peroxide and other oxidizing agents: differences between liquid and gas forms. *J. Antimicrob. Chemother.* 65:2108–2115.
- Fung-Leung WP, Kundig TM, Zinkernagel RM, Mak TW. 1991. Immune response against lymphocytic choriomeningitis virus infection in mice without CD8 expression. *J. Exp. Med.* 174:1425–1429.
- Gairin JE, Mazarguil H, Hudrisier D, Oldstone MB. 1995. Optimal lymphocytic choriomeningitis virus sequences restricted by H-2D^b major histocompatibility complex class I molecules and presented to cytotoxic T lymphocytes. *J. Virol.* 69:2297–2305.
- Guermonprez P, Valladeau J, Zitvogel L, Thery C, Amigorena S. 2002. Antigen presentation and T cell stimulation by dendritic cells. *Annu. Rev. Immunol.* 20:621–667.
- Harty JT, Tvinnereim AR, White DW. 2000. CD8⁺ T cell effector mechanisms in resistance to infection. *Annu. Rev. Immunol.* 18:275–308.
- Hombach J, Pircher H, Tonegawa S, Zinkernagel RM. 1995. Strictly transporter of antigen presentation (TAP)-dependent presentation of an immunodominant cytotoxic T lymphocyte epitope in the signal sequence of a virus protein. *J. Exp. Med.* 182:1615–1619.
- Kaech SM, Wherry EJ, Ahmed R. 2002. Effector and memory T-cell differentiation: implications for vaccine development. *Nat. Rev. Immunol.* 2:251–262.
- Kastenmüller K, et al. 2011. Protective T cell immunity in mice following protein-TLR7/8 agonist-conjugate immunization requires aggregation, type I IFN, and multiple DC subsets. *J. Clin. Invest.* 121:1782–1796.
- Kastenmüller W, et al. 2007. Cross-competition of CD8⁺ T cells shapes the immunodominance hierarchy during boost vaccination. *J. Exp. Med.* 204:2187–2198.
- Kim HW, et al. 1969. Respiratory syncytial virus disease in infants despite prior administration of antigenic inactivated vaccine. *Am. J. Epidemiol.* 89:422–434.

26. Kotturi MF, et al. 2007. The CD8+ T-cell response to lymphocytic choriomeningitis virus involves the L antigen: uncovering new tricks for an old virus. *J. Virol.* **81**:4928–4940.
27. Kotturi MF, et al. 2008. Naive precursor frequencies and MHC binding rather than the degree of epitope diversity shape CD8+ T cell immunodominance. *J. Immunol.* **181**:2124–2133.
28. La Gruta NL, et al. 2006. A virus-specific CD8+ T cell immunodominance hierarchy determined by antigen dose and precursor frequencies. *Proc. Natl. Acad. Sci. U. S. A.* **103**:994–999.
29. Lanier JG, Newman MJ, Lee EM, Sette A, Ahmed R. 1999. Peptide vaccination using nonionic block copolymers induces protective antiviral CTL responses. *Vaccine* **18**:549–557.
30. Liu F, Whitton JL, Slifka MK. 2004. The rapidity with which virus-specific CD8+ T cells initiate IFN- γ synthesis increases markedly over the course of infection and correlates with immunodominance. *J. Immunol.* **173**:456–462.
31. Matloubian M, Concepcion RJ, Ahmed R. 1994. CD4+ T cells are required to sustain CD8+ cytotoxic T-cell responses during chronic viral infection. *J. Virol.* **68**:8056–8063.
32. Moskophidis D, Cobbold SP, Waldmann H, Lehmann-Grube F. 1987. Mechanism of recovery from acute virus infection: treatment of lymphocytic choriomeningitis virus-infected mice with monoclonal antibodies reveals that Lyt-2+ T lymphocytes mediate clearance of virus and regulate the antiviral antibody response. *J. Virol.* **61**:1867–1874.
33. Murali-Krishna K, et al. 1998. Counting antigen-specific CD8 T cells: a reevaluation of bystander activation during viral infection. *Immunity* **8**:177–187.
34. Oldstone MB, et al. 1985. Virus and immune responses: lymphocytic choriomeningitis virus as a prototype model of viral pathogenesis. *Br. Med. Bull.* **41**:70–74.
35. Oldstone MB, et al. 1993. Vaccination to prevent persistent viral infection. *J. Virol.* **67**:4372–4378.
36. Pham NL, Badovinac VP, Harty JT. 2009. A default pathway of memory CD8 T cell differentiation after dendritic cell immunization is deflected by encounter with inflammatory cytokines during antigen-driven proliferation. *J. Immunol.* **183**:2337–2348.
37. Raghavan M, Del Cid N, Rizvi SM, Peters LR. 2008. MHC class I assembly: out and about. *Trends Immunol.* **29**:436–443.
38. Raué HP, Slifka MK. 2009. CD8+ T cell immunodominance shifts during the early stages of acute LCMV infection independently from functional avidity maturation. *Virology* **390**:197–204.
39. Raué HP, Slifka MK. 2007. Pivotal advance: CTLA-4+ T cells exhibit normal antiviral functions during acute viral infection. *J. Leukoc. Biol.* **81**:1165–1175.
40. Rock KL, Shen L. 2005. Cross-presentation: underlying mechanisms and role in immune surveillance. *Immunol. Rev.* **207**:166–183.
41. Rodriguez F, Slifka MK, Harkins S, Whitton JL. 2001. Two overlapping subdominant epitopes identified by DNA immunization induce protective CD8(+) T-cell populations with differing cytolytic activities. *J. Virol.* **75**:7399–7409.
42. Seder RA, Darrah PA, Roederer M. 2008. T-cell quality in memory and protection: implications for vaccine design. *Nat. Rev. Immunol.* **8**:247–258.
43. Shen H, et al. 1995. Recombinant *Listeria monocytogenes* as a live vaccine vehicle for the induction of protective anti-viral cell-mediated immunity. *Proc. Natl. Acad. Sci. U. S. A.* **92**:3987–3991.
44. Shin H, Wherry EJ. 2007. CD8 T cell dysfunction during chronic viral infection. *Curr. Opin. Immunol.* **19**:408–415.
45. Sigal LJ, Rock KL. 2000. Bone marrow-derived antigen-presenting cells are required for the generation of cytotoxic T lymphocyte responses to viruses and use transporter associated with antigen presentation (TAP)-dependent and -independent pathways of antigen presentation. *J. Exp. Med.* **192**:1143–1150.
46. Slifka MK, et al. 1996. Antiviral cytotoxic T-cell memory by vaccination with recombinant *Listeria monocytogenes*. *J. Virol.* **70**:2902–2910.
47. Slifka MK, Whitton JL. 2000. Activated and memory CD8+ T cells can be distinguished by their cytokine profiles and phenotypic markers. *J. Immunol.* **164**:208–216.
48. Speidel K, et al. 1997. Priming of cytotoxic T lymphocytes by five heat-aggregated antigens in vivo: conditions, efficiency, and relation to antibody responses. *Eur. J. Immunol.* **27**:2391–2399.
49. Sun Y, Santra S, Schmitz JE, Roederer M, Letvin NL. 2008. Magnitude and quality of vaccine-elicited T-cell responses in the control of immunodeficiency virus replication in rhesus monkeys. *J. Virol.* **82**:8812–8819.
50. Takagi A, et al. 2009. Highly efficient antiviral CD8+ T-cell induction by peptides coupled to the surfaces of liposomes. *Clin. Vaccine Immunol.* **16**:1383–1392.
51. Tebo AE, et al. 2005. Rapid recruitment of virus-specific CD8 T cells restructures immunodominance during protective secondary responses. *J. Virol.* **79**:12703–12713.
52. Tewari K, Sacha J, Gao X, Suresh M. 2004. Effect of chronic viral infection on epitope selection, cytokine production, and surface phenotype of CD8 T cells and the role of IFN- γ receptor in immune regulation. *J. Immunol.* **172**:1491–1500.
53. van der Most RG, et al. 1998. Identification of Db- and Kb-restricted subdominant cytotoxic T-cell responses in lymphocytic choriomeningitis virus-infected mice. *Virology* **240**:158–167.
54. Walsh CM, et al. 1994. Immune function in mice lacking the perforin gene. *Proc. Natl. Acad. Sci. U. S. A.* **91**:10854–10858.
55. Wherry EJ, Blattman JN, Murali-Krishna K, van der Most R, Ahmed R. 2003. Viral persistence alters CD8 T-cell immunodominance and tissue distribution and results in distinct stages of functional impairment. *J. Virol.* **77**:4911–4927.
56. Wherry EJ, et al. 2003. Lineage relationship and protective immunity of memory CD8 T cell subsets. *Nat. Immunol.* **4**:225–234.
57. Whitmire JK, Eam B, Benning N, Whitton JL. 2007. Direct interferon- γ signaling dramatically enhances CD4+ and CD8+ T cell memory. *J. Immunol.* **179**:1190–1197.
58. Whitmire JK, Tan JT, Whitton JL. 2005. Interferon- γ acts directly on CD8+ T cells to increase their abundance during virus infection. *J. Exp. Med.* **201**:1053–1059.
59. Whitton JL, Slifka MK, Liu F, Nussbaum AK, Whitmire JK. 2004. The regulation and maturation of antiviral immune responses. *Adv. Virus Res.* **63**:181–238.
60. Yamamoto N. 1969. Damage, repair, and recombination. II. Effect of hydrogen peroxide on the bacteriophage genome. *Virology* **38**:457–463.
61. Yewdell JW, Bennink JR. 1999. Immunodominance in major histocompatibility complex class I-restricted T lymphocyte responses. *Annu. Rev. Immunol.* **17**:51–88.
62. Yoshimura Y, et al. 2004. Duration of alloantigen presentation and avidity of T cell antigen recognition correlate with immunodominance of CTL response to minor histocompatibility antigens. *J. Immunol.* **172**:6666–6674.
63. Yu TW, Anderson D. 1997. Reactive oxygen species-induced DNA damage and its modification: a chemical investigation. *Mutat. Res.* **379**:201–210.
64. Zajac AJ, et al. 1998. Viral immune evasion due to persistence of activated T cells without effector function. *J. Exp. Med.* **188**:2205–2213.